Journal of
Nanoscience and Nanotechnology
Vol. 9, 5981–5989, 2009

# Induced Secondary Structure in Nanostructured Films of Poly(*p*-phenylene vinylene)

Paulo Alliprandini-Filho[1], George B. da Silva[2], Newton M. Barbosa Neto[1], R. A. Silva[1], and Alexandre Marletta[1,*]

[1] *Instituto de Física–Universidade Federal de Uberlândia, C. P. 359, 38400-902, Uberlândia–MG, Brazil*
[2] *Universidade Federal do Mato Grosso, 78698-000, Pontal do Araguaia–MT, Brazil*

The control of emission properties in luminescent polymers such as poly(*p*-phenylene vinylene) (PPV) is important for various applications, and may be achieved with suitable molecular architectures in nanostructured films. This paper reports on optical properties of PPV films, using ellipsometry measurements for emitted light in the scope of the Stokes' theory. Organized PPV films obtained with the Langmuir-Blodgett (LB) method exhibited high degree of polarization for the emitted light, while cast films emitted mainly non-polarized light. From ellipsometry data, a secondary structure was inferred for poly(xylylidene tetrahydrothiophenium) chloride (PTHT), a PPV precursor, in solution, which is retained only to a small extent in the PPV cast film as thermal conversion was performed close to the glass transition temperature of PPV. On the other hand, a higher intensity of emitted light with circular polarization was observed for the LB film, which is attributed to PPV molecular secondary structure that was enhanced during the LB film deposition. Circular dichroism experiments were performed to corroborate this hypothesis. It is suggested that such a secondary structure has not been predicted in theoretical models for PPV because possible conformational changes induced in the processing steps are not taken into account.

**Keywords:** Poly(*p*-phenylene vinylene), Ellipsometry, Stokes' Theory, Langmuir-Blodgett Films.

## 1. INTRODUCTION

Luminescent polymers have been studied as active layers in polymer light-emitting diodes (PLEDs),[1,2] where control of emitted light polarization may be exploited in the information industry.[3] In order to develop such new technologies, however, a correlation has to be established between molecular structure and electronic and optical properties, which is still an open problem. For conjugated polymers, in particular, several issues related to molecular organization must be addressed. Using molecular engineering strategies, chiral or oriented molecules can be produced, e.g., with incorporation of lateral groups along the polymer main chain of poly(*p*-phenylene vinylene) (PPV).[4] With this procedure, emission of circularly polarized light was observed with an asymmetry parameter ($g$) of $5 \times 10^{-3}$ and $1.7 \times 10^{-3}$ for poly(*p*-phenylene) and PPV, respectively.[5,6] The asymmetry was interpreted as consequence of the secondary structure (or molecular conformation) induced by lateral groups. Verbiest et al.[7,8] suggested that oriented, non-chiral molecules may also exhibit optical activity when the experimental geometry is not symmetric. This occurs in spectroscopic measurements when the wave vector of the incident light, the orientation axis of the molecule and the wave vector of scattered or emitted light form a non-coplanar configuration. Another example is the formation of molecular aggregation caused by interaction between side chains, which was observed in solid-state phase and in solutions using a weak solvent,[9,10] yielding the Cotton effect. Optical activity in molecules is normally associated with the molecular secondary structure and the presence of asymmetric carbon. However, a convenient arrangement of non-chiral molecules can break the molecular symmetry,[4] as may be the case of Langmuir-Blodgett films.[11]

PPV films are commonly obtained from the soluble precursor poly(xylylidene tetrahydrothiophenium) chloride (PTHT), which is then thermally converted into PPV. Thermal conversion is usually performed at high temperatures (~250 °C) under vacuum and during long times (~6 h), but an alternative route was proposed by Marletta et al.[12] whereby conversion was possible at considerably lower temperatures and short times, by exchanging the chlorine counter-ion with the dodecylbenzenesulphonic

*Author to whom correspondence should be addressed.

(DBS) counter-ion. This new route facilitates inclusion of hydrophobic lateral groups in the PTHT polyelectrolyte to produce stable Langmuir films. Transfer of these PTHT films onto solid substrates led to Z-type LB films that could be converted into PPV at (~110 °C). The resulting LB PPV/DBS films were anisotropic, with molecular alignment on the film plane,[13] for which the emitted light was linearly polarized (ca. 70%) and a circular dichroism (CD) signal of ca. 100 mdeg was measured.[14] These values are one order of magnitude greater than for a cast PPV film. However, in solid state the CD signal may arise from circular birefringence, and may not be directly related to the conformation molecular structure.

In this study we performed ellipsometry measurements to probe the total polarization state of the emitted light from ordered and non-ordered PPV films, which is not possible using the conventional experiment with linear polarizers. Our results can be explained by assuming that DBS counter-ions and the film processing with the LB technique induce a secondary structure for PPV chains. We shall also discuss why a possible secondary structure for PPV has not been predicted in theoretical models.[15]



## 2. EXPERIMENTAL DETAILS

The chemical synthesis of PPV was performed using a soluble precursor polymer (PTHT) as described in Ref. [16]. The cast and LB-PPV films were produced following the procedures in Ref. [13], being deposited onto hydrophobic glass substrates (BK7). The Z-type LB film made with PTHT had 40 layers with transfer ratios of 0.8 for upstrokes and 0.3 for the downstrokes. For fabricating the LB film, DBS molecules were added in the PPV precursor polymer solution at a 1:1 wt/wt in 1,2-dichlorometane-ethanol (1:1 v/v) solution, thus replacing the Cl counter-ions to impart hydrophobic characteristics to PTHT and obtain stable Langmuir films at the air/water interface. Cast PTHT films were prepared after solvent evaporation at room temperature (~25 °C), with a thickness of 0.9 $\mu$m. PTHT/DBS LB and PTHT cast films were then thermally converted at 200 °C under vacuum ($10^{-2}$ atm) for 2 hours, resulting in LB-PPV and cast PPV films.

The absorbance spectra in the UV-vis region were obtained with a homemade assembly, using a deuterium-tungsten lamp from Ocean Optics model DTmini as light source. The transmitted light through the sample was acquired by a USB2000 Ocean Optics CCD spectrometer. Circular Dichroism measurements were carried out with a Jasco Spectropolarimeter J-720. For photoluminescence (PL) measurements, the samples were excited with an Argon ion laser, model Stabilite 2017, from spectra Physics Inc. at 458 nm (2.71 eV) and 488 nm (2.54 eV). The emitted light was guided by a set of lenses into the USB2000 Ocean Optics spectrometer. Low pass filters, with cutoff at 475 nm and 515 nm, were placed in front of the spectrophotometer to cut the corresponding excitation wavelengths.

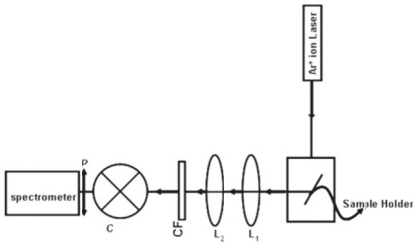


**Fig. 1.** Experimental setup for ellipsometry measurements. $L_1$ and $L_2$ are lenses, CF is the cutoff filter, C is the compensator and P is the fixed polarizer.

In polarized photoluminescence measurements, two polarizers were inserted into the experimental setup: the first one was positioned between the laser source and the sample, while the second polarizer was placed between the sample and the spectrophotometer. In all photoluminescence experiments, the samples were placed in a He closed-cycle cryostat that allows one to perform measurements at very low (10 K) and room (300 K) temperatures. The linear birefringence experiment was performed using one He–Ne laser and two polarizers.

Figure 1 shows the experimental setup for the ellipsometry measurements. A quarter wave plate was inserted in the setup employed for measuring photoluminescence as a compensator, while a polarizer was introduced before the spectrometer. Both films were positioned on the plane perpendicular to the optical path of the emitted light. Two compensators were used, at 543 nm and 633 nm. The luminescence was guided through the set of $L_1$ and $L_2$ lenses, the high pass filter (>475 nm-CF), the quarter wave plate (compensator-C), polarizer (P), and the spectrometer. With a goniometer the compensator was rotated from 0° to 360° around the axis parallel to the optical path of emitted light, in steps of 10°.

## 3. RESULTS AND DISCUSSION

### 3.1. Film Anisotropy and Emission of Polarized Light

Figure 2 shows the absorbance spectra for a cast PPV film for different polarizations of the transmitted light: (i) non-polarized, (ii) parallel polarization (vertical polarization), and (iii) perpendicular polarization (horizontal polarization). The film exhibits strong absorption between 350 and 525 nm, assigned to transitions between non-localized $\pi \rightarrow \pi^*$ states. According to the molecular exciton model,[17] the broad band is due to PPV segments with different sizes. The position of the maximum (~439 nm), the bandwidth and the absorbance at the edge ($\lambda_{edge}$ = 502 nm) are not affected by the polarization of the transmitted light, which indicates that the film has a uniform, random distribution of PPV chains, as expected. Quantitative information on molecular ordering in the film plane

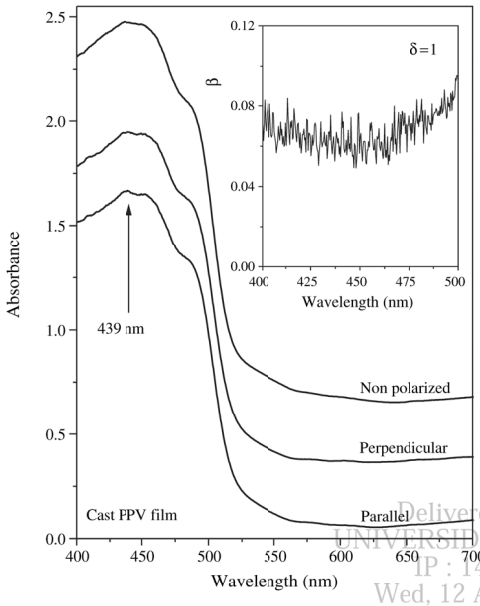


**Fig. 2.** Absorption spectra for cast PFV film with various polarizations of the transmitted light. The spectra were shifted upward to facilitate visualization. In the insert, the $\beta$ parameter is given versus wavelength.

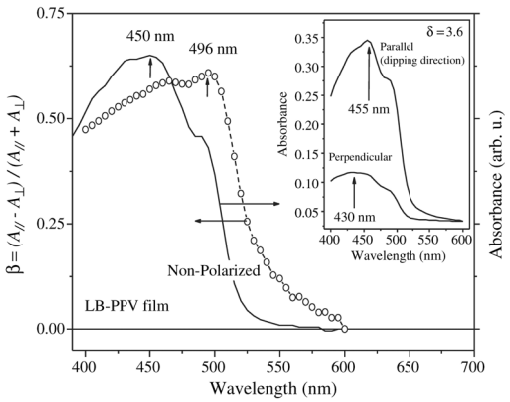


**Fig. 3.** $\beta$ factor and absorption spectrum with non-polarized light for an LB-PPV film. The spectra for an LB-PPV film for different polarizations of the transmitted light were reproduced with permission from [13], A. Marletta et al., *Macromolecules* 33, 5886 (**2000**). © 2000, and given in the insert.



is obtained by analyzing the molecular order parameter ($\beta$), which is defined as $\beta = (A_{//} - A_{\perp})/(A_{//} + A_{\perp})$, extracted from the polarized absorption spectra. $A_{//}$ is the absorbance intensity for parallel (or vertical) and $A_{\perp}$ is the absorbance intensity for perpendicular (or horizontal) polarization of the transmitted light. The $\beta$ value, calculated in the absorption band range, is approximately constant, ~0.07, as shown in the insert of Figure 2. This confirms the random orientation of PPV molecules on the substrate, which is corroborated by a dichroic ratio ($\delta$) of ~1. Despite the isotropic orientation, there is a slight increase in $\beta$ at the edge of the absorption band, which is related to large conjugated PPV segments that tend to self-organize. Above 500 nm, the calculation of this parameter was not possible due to the low absorbance values. The positive $\beta$ points to a small asymmetry, which is frequently observed in cast films, regardless of film thickness.

The absorption spectrum and $\beta$ parameter for the LB-PPV film are shown in Figure 3. The LB-PPV film exhibits an absorption band between 400 to 550 nm assigned to non-localized transitions ($\pi \rightarrow \pi^*$). In comparison with the cast film, the spectrum is less intense in the blue region, owing to a smaller concentration of PPV segments of low conjugation degrees. On the other hand, the spectra depend strongly on the light polarization state, as shown in the insert of Figure 3, extracted from Ref. [13]. The dichroic ratio was 3.6, and the absorption maximum was red shifted by ca. 25 nm for the parallel polarization (dipping direction). In addition, the spectrum is better defined with lower intensity at small wavelengths than for the cast film. This indicates that the PPV segments with larger conjugation lengths are preferentially aligned in the parallel (or dipping) direction. Hence, the alignment of polymer chains is largely determined by the dipping process while transferring the Langmuir PTHT film.[13] The spectrum for the parallel polarized light is narrower because there is less dispersion in the sizes of conjugated PPV segments in the dipping direction. Indeed, $\beta$ has a large positive value, approximately 0.6 with maximum at 496 nm.

Since the refractive index, $n$, in conjugated polymers may depend on the degree of conjugation, a linear birefringence was expected. We estimated the birefringence by measuring the transmitted light through PPV films, with a He–Ne laser (633 nm) probe beam. The sample was placed in the optical path between polarizers rotated at 45° and −45° in relation to the vertical axis (laboratory framework or dipping direction). The signal was detected as a function of the rotational angle $\theta$ ($0 \leq \theta \leq 2\pi$) of the sample in relation to the vertical axis. Figure 4 shows the result for the LB-PPV film, with the data being fitted with the following expression:

$$\frac{I}{I_o} = \sin^2\left(\frac{\pi L}{\lambda_0}\Delta n\right) \quad (1)$$

where $L$ is the mean thickness, approximately 100 nm for the LB-PPV film, $\lambda_o$ is the wavelength of the light transmitted (633 nm) and $\Delta n (= n_{//} - n_{\perp})$ is the difference between the refraction index in the parallel ($n_{//}$) and perpendicular ($n_{\perp}$) directions. From the fitting $\Delta n = 3.1 \times 10^{-2}$ for the LE sample, which is compatible with LB films of azodye polymers used in optical storage devices.[18] For cast PPV film, $\Delta n$ was negligible.

Figures 5(a) and (b) show the photoluminescence spectra with excitation at 458 nm for cast and LB PPV films,

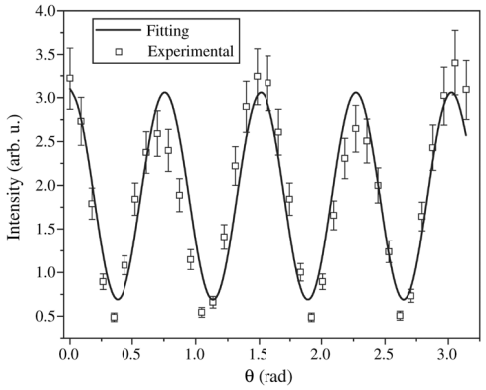


**Fig. 4.** Transmitted light versus angle of rotation of the analyzer (2nd polarizer), from which the birefringence was estimated for an LB-PPV film. The solid line is the theoretical fitting obtained with Eq. (1).



at 10 K and 300 K, respectively. Similar results were obtained with excitation by laser light at 488 nm (results not shown). The arrows at 543 and 633 nm indicate where the PL intensity was measured in the ellipsometry experiments (see later). Generally, three emission peaks associated with electronic transition (LUMO–HOMO transition) and coupling of vibrational modes are observed. The typical vibrational modes appear at 500, 1100 and 1550 $cm^{-1}$ assigned to C–H and C–C ring out-of-plane bend, C–H ring in-plane-bend and C–C ring stretch, respectively.[19, 20] The spectrum is better defined for the LB-PPV film, owing to the higher ordering of polymer chains and reduced interchain interaction with DBS ions in the LB-PTHT film. These data are consistent with the red shift in the absorbance spectrum of the LB-PPV film and with PPV segments with larger conjugation degree and less energy dispersion than the cast PPV film (see Figs. 2 and 3).

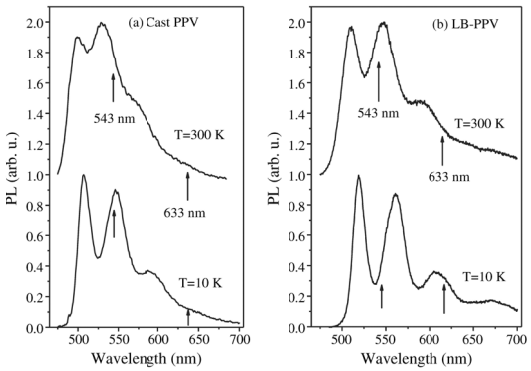


**Fig. 5.** Photoluminescence for (a) cast PPV and (b) LB-PPV films at 10 K and 300 K. The wavelengths probed in the ellipsometry experiments are indicated with arrows: 543 and 633 nm. The curves were normalized and shifted vertically to facilitate visualization.

The PL line shape is better defined at low temperatures owing to a decreased thermal disorder. Also from Figure 5, we note that the increase in temperature causes the peaks to be shifted to smaller wavelengths, with the ratio between the intensities of transitions at ~500 nm and first vibrational mode at ~540 nm increasing by 11% for the cast film and 4% for the LB film. This modification in line shape is caused by two effects: (i) decrease in effective conjugation degree of PPV segments and (ii) increase in thermal disorder.[21] The change in the peak intensity ratio is explained by an increase in coupling of electron-vibrational modes.[17] In addition, raising the temperature causes a decrease in PL intensity due to an increased activation of non-radiative decay paths.[13] The line shape for the cast PPV film (Fig. 5(a)) is more strongly affected by the temperature than the LB-PPV film (Fig. 5(b)). This appears to indicate that molecules in the LB film are more rigidly arranged, being less susceptible to changes with the temperature.

The degree of polarization of the emitted light was investigated by positioning a polarizer that rotates 360°, in steps of 20°, around the axis parallel to the optical path. If the emitted light were completely non-polarized and/or circularly polarized, it should not depend on the polarizer rotation angle $\theta$ (formed between the vertical direction, parallel to the dipping direction, and the polarization axis). If there is some polarization, the emission intensity versus angle should obey the Mallus' law:

$$I(\theta) = I' \cos^2(\theta - \alpha) + I_o \quad (2)$$

where $I_0$ is the correction term that takes into account non-polarized and/or circular polarized light, $\alpha$ is a constant phase and $I'$ is the intensity of the emitted light with linear polarization. If the light has just linear polarization, $I_0$ is null, and the original Mallus' law is obtained. The experiments were carried out by exciting the films with laser polarization in the parallel and perpendicular directions using the 458 nm and 488 nm wavelengths. Emission was analyzed at 510, 543, 613, and 633 nm, for sample temperatures of 10 K and 300 K.

Figure 6 shows the data for the cast and LB-PPV samples, with excitation at 458 nm with parallel polarization and analyzing the PL signal at 510 nm and room temperature. Similar results (not shown) were obtained exciting the sample with perpendicular polarization. It is worth noting that despite the molecular disorder in the cast film, there is a small portion of polarized light, which is consistent with $\beta$ from Figure 2. This is indicative that PPV films obtained from a precursor polymer (PTHT) exhibit some self-organization. For the LB-PPV film, the emitted light exhibits high contents of linear polarization, for all wavelengths studied. This is due to the anisotropy, which was even higher than for the parallel direction. For excitation at the perpendicular direction, energy transfer and/or carrier migration occurs to segments with conjugation in

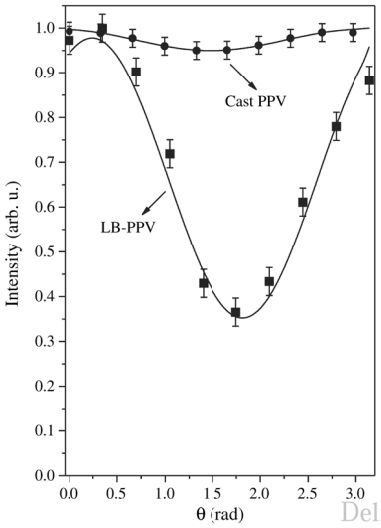


**Fig. 6.** Measurement of the angle dependence for emission of cast and LB-PPV films. The samples were excited at 458 nm with parallel polarization, and the emitted light was measured at 510 nm. The solid line is the theoretical fitting obtained using Eq. (2), for room temperature.



the parallel direction (from high to low gap energy).[13, 22] This result is corroborated by the presence of PPV segments with small conjugation degree in the perpendicular direction, which was inferred from the absorption spectrum and positive $\beta$ in Figure 3. In subsidiary experiments, we verified that the results depicted in Figure 6 for LB and cast films did not depend on the sample temperature or on the wavelength at which emission was detected. The lack of temperature dependence may be explained by the high glass transition temperature ($T_g$) of PPV, which is ca. 200 °C. At the temperatures used in the experiment the polymer chains did not have sufficient thermal energy and/or free volume for changes in their macroscopic orientation and in the transition moment for emission.

The solid lines in Figure 6 represent the fitting of experimental data using Eq. (2). Table I summarizes the fitting parameters $I'$, $I_0$ and $\alpha$ for data with distinct polarizations of the excitation beam and emission at 510 nm. For the cast film emission light is not polarized ($I' \ll 1$) for neither of the exciting polarizations, again consistent with $\beta$ (ca. 0.07) in Figure 2. For the LB-PPV film in the emission wavelengths analyzed, light is ~64% linearly polarized in parallel direction, for both excitation in the parallel and perpendicular direction. Therefore, a greater percentage of polarized light is emitted with the parallel excitation owing to the preferential alignment of polymer chains in this direction ($\beta \approx 0.6$ at 496 nm-Fig. 3). However, with the Mallus' law experiment one is not able to determine the polarization state related with $I_0$, for linear polarizers are not appropriate to analyze circular and/or random polarization in solid state films. Such analysis is made possible with ellipsometry experiments described below.

**Table I.** Parameters for cast and LB-PPV films obtained using Eq. (2). The samples were excited at 458 nm and the PL intensity was detected at 510 nm. For the LB film, both the parallel and perpendicular polarizations of the exciting beam were used.

| PPV film | Excitation polarization | $\lambda_{em}$ (nm) | $I'$ (a.u.) | $I_0$ (a.u.) | $\alpha$ (degrees) |
|---|---|---|---|---|---|
| Cast | Parallel | 510 | 0.05 | 0.95 | −5.2 |
| LB | Parallel | 510 | 0.63 | 0.35 | 13.9 |
| | Perpendicular | 510 | 0.67 | 0.31 | 12.5 |

To quantify the influence of molecular ordering and packing in the film plane on the polarization state of the luminescence, we introduce the anisotropy factor $r$ defined as:[23]

$$r = \frac{I_{//,//} - GI_{//,\perp}}{I_{//,//} + 2G_{//,\perp}} \quad (3)$$

where $G = I_{\perp,//}/I_{\perp,\perp}$. The intensities ($I_{Ex,Em}$) are taken from polarized luminescence measurements (not shown here) performed with cast and LB-PPV films, in the four possible polarization configurations for excitation (Ex) and emission (Em): parallel (//) and perpendicular ($\perp$). Figure 7 displays $r$ versus wavelength at the emission range. For the cast PPV film, $r$ is close to zero as the film is isotropic, consistent with results from polarized absorption (Fig. 2) and polarization of emitted light (Fig. 6). For the LB-PPV film, $r$ increases substantially up to 0.95, thus demonstrating the high molecular ordering. Furthermore, $r$ is practically independent of the wavelength in the range of phonon replicas, which indicates that the coupling of electron–phonon is not able to introduce anisotropy by thermal disorder.

### 3.2. Emission of Circularly Polarized Light and Induced Secondary Structure of PPV

Although the Mallus' experiment with results depicted in Figure 6 gives the extent of linear polarization in

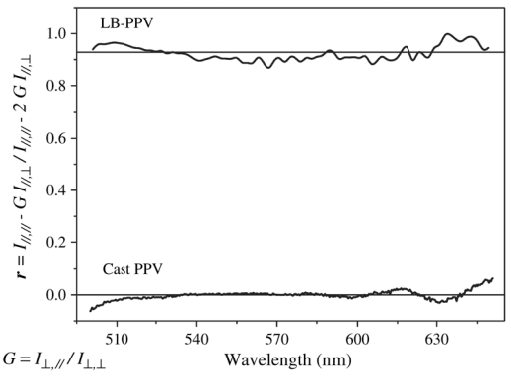


**Fig. 7.** Anisotropy parameter $r$ in the UV-Vis region for cast and LB-PPV films.

fluorescence, it is not able to provide information on the state of polarization (linear, circular and random polarization) of emitted light. Ellipsometry experiments were then carried out to determine this state of polarization for cast and LB films, for which use was made of the Stokes' theory for the electromagnetic field.[24] The measurements were performed at 10 K and 300 K to study thermal disorder effects. We used the excitation at 458 nm and 488 nm to probe the influence from energy transfer between PPV segments (inter band transitions), and the emission was detected at 543 and 633 nm to verify the influence from coupling with vibrational modes (intra-band transitions). The polarization of the excitation light was set to parallel and perpendicular to infer about the possible arrangements for the PPV molecules on the film plane. The Stokes parameters for the electric field were obtained by fitting the ellipsometry data with Eq. (4).[24, 25]

$$I(\theta) = \frac{1}{2}[A + B\sin(2\theta) + C\cos(4\theta) + D\sin(4\theta)] \quad (4)$$

where $I$ is proportional to the electric field intensity, $\theta$ is the angle between the fast axis of the quarter wave plate and the axis of the polarizer (vertical direction), $A = S_0 + (S_1/2)$, $B = S_3$, $C = S_1/2$, and $D = S_2/2$. $S_0$, $S_1$, $S_2$ and $S_3$ are the Stokes parameters that describe the polarization state of the emitted light. $S_0$ is associated with the total intensity of the optical field, $S_1$ describes the quantity of linear polarization on the parallel or perpendicular directions, $S_2$ gives the quantity of linear polarization rotated by $+45°$ or $-45°$, and $S_3$ provides information on the existence of right or left circularly polarized light, respectively.

Figures 8(a) and (b) display ellipsometry curves for cast and LB films, respectively, at 300 K, with the samples being excited at 458 nm with parallel polarization and analyzing the signal at 543 nm. Figure 8(c) shows the result for the LB film excited with perpendicular polarization at 300 K. The solid lines represent the fittings of the experimental data with Eq. (4). In addition to the Stokes parameters, the asymmetry factor $g$ reveals the difference between the emitted light with right- and left-circular polarizations, defined as:[24, 25]

$$g = 2\frac{I_L - I_R}{I_L + I_R} \quad (5)$$

where $I_L$ and $I_R$ are the light intensity obtained for $\alpha + 45°$ and $\alpha - 45°$, respectively, and $\alpha$ is the same factor of Table I.

Table II shows the normalized Stokes parameters and $g$ factor from the fitting of experimental data in Figure 8. Due to the disorder in the cast film, excitation with different polarizations did not change the results. The parameter $S_1/S_0$ is rather low, consistent with $I'$ obtained in the experiment of Figure 6. The factor $g$ is small, ca. $10^{-3}$, but not null. This small portion of circularly polarized emitted

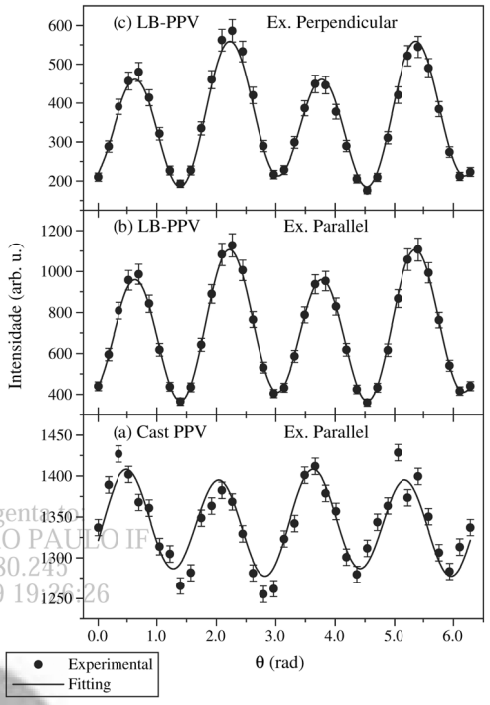


**Fig. 8.** (a) Results from the ellipsometry experiment at 300 K for cast PPV, exciting the sample at 458 nm with parallel polarization and analyzing the emitted light at 543 nm at 300 K. The same for the LB-PPV film exciting the sample at 458 nm with (b) parallel and (c) perpendicular polarization; the emitted light was analyzed at 543 nm. The solid curves are fittings obtained with Eq. (4).

light was not expected for PPV which is believed to adopt a planar symmetry.[15] Similar results were observed in optical activity experiments for polythiophenes with lateral groups and nematic fluids with chiral molecules.[5] For PPV, circularly polarized emission was reported but with chiral molecules being added as lateral groups along the main polymer chain, with asymmetry parameter of $1.7 \times 10^{-3}$.[5]

For the LB film, when the sample was excited with parallel polarization, the normalized parameter $S_1/S_0$ was higher than for the cast film, again consistent with the results in Figure 6. Its negative value means that the polarization of the emitted light is preferentially in the parallel direction. The $S_1/S_0$ values in Table II show that the percentage of emitted light with linear polarization for the LB film does not depend on the polarization of the exciting beam, being approximately 64% for all experimental conditions. This is consistent with the discussion for the results in Figure 6, where emission was taken to be proportional to the number of PPV segments in the parallel direction, regardless of the excitation polarization. The parameter $S_2/S_0$ is also large for the LB-film, indicating that the emitted light is rotated in relation to the

**Table II.** Stokes parameters $S_0$, $S_1$, $S_2$ and $S_3$ and $g$ factor for cast and LB-PPV films at 10 K and 300 K. The samples were excited at 458 nm and the PL intensity was detected at 543 nm and 633 nm. For the LB film, both the parallel and perpendicular polarizations of the exciting beam were used.

| $\lambda/4$ (nm) | $T$(K) | $S_1/S_0$ | $S_2/S_0$ | $S_3/S_0$ | $g$ |
|---|---|---|---|---|---|
| Cast PPV film: Perpendicular excitation | | | | | |
| 543 | 10 | −0.01 | 0.06 | −0.006 | 0.001 |
| | 300 | −0.03 | 0.08 | −0.006 | 0.001 |
| 633 | 10 | −0.03 | 0.10 | −0.006 | 0.001 |
| | 300 | −0.05 | 0.13 | −0.006 | 0.001 |
| LB-PPV film: Parallel excitation | | | | | |
| 543 | 10 | −0.55 | 0.34 | −0.10 | 0.17 |
| | 300 | −0.56 | 0.36 | −0.08 | 0.13 |
| 633 | 10 | −0.63 | 0.32 | −0.04 | 0.07 |
| | 300 | −0.56 | 0.41 | −0.02 | 0.04 |
| LB-PPV film: Perpendicular excitation | | | | | |
| 543 | 10 | 0.56 | 0.21 | 0.01 | 0.02 |
| | 300 | 0.59 | 0.26 | 0.03 | 0.05 |
| 633 | 10 | 0.61 | 0.11 | 0.01 | 0.04 |
| | 300 | 0.64 | 0.23 | 0.01 | 0.02 |



laboratory framework. This is due to the linear birefringence properties of the LB-PPV film observed in Fig. 4. The parameter $S_3/S_0$ and the asymmetry factor $g$ depend, surprisingly and strongly, on the wavelength for analysis. It is two orders of magnitude higher in the LB film than in the cast film for 543 nm, but one order higher of magnitude for 633 nm. It is clear that the coupling of electron–phonon plays an important role; see the PL spectra in Figure 5. The possible explanation for the dependence of $g$ with the wavelength and film processing is the symmetry breaking of supposedly planar PPV molecules, thus introducing a new conformational structure.

For the LB-PPV film, DBS molecules along the PTHT polymer could induce a new conformation for PTHT/DBS polymer with chiral structure due to the steric interaction between adjacent monomers. If there is a chiral conformation for LB PPV/DBS chains, the vibrational modes induce thermal disorder in the molecular structure and the parameter $g$ (or $S_3/S_0$) decreases. This explains why $g$ is higher for radiative transition next to the zero-phonon peak (543 nm). The lack of dependence of $g$ on the excitation wavelength in the perpendicular direction is due to an increased electron–phonon coupling (or Huang-Rhys parameter–$S$) as reported in Ref. [13]. In other words, thermal disorder introduced during carrier migration from perpendicular to parallel direction decreases the portion of emitted light with circular polarization. In addition, there is practically no temperature dependence for $g$ in either polarization directions of the exciting beam. These results demonstrate that the chiral structure induced in the LB film has a stable configuration with energy of ca. 100 meV, i.e., the phonon energy for PPV associated with the emission wavelength at 633 nm. For the cast PPV film, on the other hand, the low $g$ and the thermal stability support the presence of chiral structures with configuration energy higher than 25 meV ($kT$ at room temperature) and less than 60 meV (phonon energy at 543 nm). Finally, the fitting parameters (not shown) obtained when the cast and LB-PPV films are excited at 488 nm are similar to those for 458 nm. This shows that the emitted light does not depend strongly on the inter-band transition during energy transfer and/or carriers diffusion.

Since emitted light had circular polarization for both samples, although with different intensities, it cannot be attributed solely to film architecture. To verify the possibility that the films present circular birefringence, we measured the circular dichroism, whose results are shown in Figure 9. The curves display a line shape similar to that for absorption (Figs. 2 and 3) in the spectral range associated with $\pi \rightarrow \pi^*$ transitions. The CD signal is zero above 500 nm for the cast and 550 nm for the LB-PPV film.

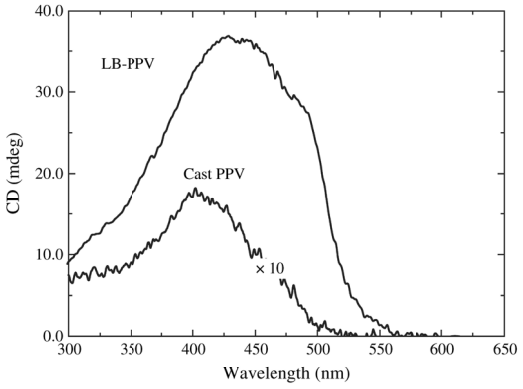


**Fig. 9.** Circular dichroism curves for cast and LB-PPV samples in the UV-Vis region.

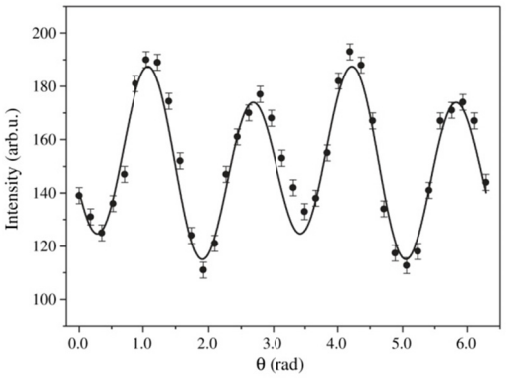


**Fig. 10.** Ellipsometry experiment for PTHT polymer in solution at 300 K. The sample was excited at 458 nm with parallel polarization and the emitted light was analyzed at 543 nm. The solid curves are the fitting obtained with Eq. (4).



Hence, the films do not present circular birefringence in the emission wavelength range analyzed, which indicates that circular emission in the ellipsometry experiment has to be associated with the conformational structure (or secondary structure) of PPV molecules.

The secondary structure of PTHT (PPV precursor) in aqueous solution was obtained from ellipsometry measurements at 543 nm in Figure 10. From fitting the Stokes parameters, $g = 0.03$, one order of magnitude greater than for the cast film (see Table II). The small $g$ for the cast film could be attributed to the PPV synthesis route at high temperature (200 °C), which is close to the PPV glass transition temperature. In this case, film processing produces a random, disordered structure and increases entanglement between polymer chains. For the LB films, in contrast, the secondary structure of PPV could be enhanced by the Z-type film structure where the adjacent PPV layers are separated by DBS molecules.

The chemical structure of PPV has inversion symmetry, which implies that this molecule should be tunable to produce circularly polarized light emission. This statement applies to pristine PPV polymer, for which theoretical calculations have been done.[15] However, it is possible that Coulomb and/or van der Waals interactions may induce conformational changes in the precursor polyelectrolyte polymer chains during the PPV film processing. Furthermore, effects could arise from the stilbene moieties (short PPV segments) in PTHT.

It may not be surprising that a secondary structure in PPV has not been captured in theoretical models, as the latter do not consider some processing steps and that the final sample may be made of copolymers of fully converted PPV and non-converted PTHT. Therefore, further ingredients must be added to theoretical modeling in order to match the experimental conditions under which PPV films are produced.

## 4. CONCLUSIONS

We have used ellipsometry measurements to probe the polarization state of PPV films and try to determine the possible origins for emission of circularly polarized light. It was found that molecules of PTHT, the PPV precursor, in solution already exhibited a secondary structure (such as helices), but this structuring was mostly lost in cast PPV films owing to the film processing step carried out at a high temperature, close to $T_g$. This secondary structure inherent in PTHT was maintained (and enhanced) in an LB film, even after thermal conversion, probably due to the anisotropy induced by the film-forming technique. The anisotropy was probed with absorption and emission spectra, with excitation polarized in both parallel and perpendicular directions to the dipping direction. Important in this context was the energy transfer (or exciton migration) among PPV chains, from the large band gap to the small band gap segments. From the results shown, we suggest that efforts should be done to develop new molecular engineering strategies to manipulate polymer chains during the synthesis, in addition to the possible identification of suitable energy (or charge) donor–acceptor pairs.[26] For emission of circularly polarized light, in particular, strategies should focus on a way to break the symmetry of polymeric chains.

**Acknowledgments:** The authors are grateful to the Brazilian Agencies (CNPq and FAPEMIG) and MCT/IMMP for financial support. We are also indebted to Professor Noélio O. Dantas, from *Instituto de Física* of *Universidade Federal de Uberlândia*, Brazil, for the use of experimental facilities.

## References and Notes

1. R. H. Friend, G. J. Denton, J. J. M. Halls, N. T. Harrison, A. B. Holmes, A. Köhler, A. Lux, S. C. Moratti, K. Pichler, N. Tessler, K. Towns, and H. F. Wittmann, *Solid State Commun.* 102, 249 **(1997)**.
2. S. Xiong, S. H. Huang, A. W. Tang, and F. Teng, *J. Nanosci. Nanotechnol.* 8, 1341 **(2008)**.
3. V. Cimrová, R. Marcus, D. Neher, and G. Wegner, *Adv. Mater.* 8, 146 **(1997)**.
4. R. Viswanathan, J. A. Zasadzinski, and D. K. Schwartz, *Nature* 368, 440 **(1994)**.
5. E. Peeters, M. P. T. Christiaans, R. A. J. Janssen, H. F. M. Schoo, H. P. J. M. Dekkers, and E. W. Meijer, *J. Am. Chem. Soc.* 119, 9909 **(1997)**.
6. R. Fiesel and U. Scherf, *Macromol. Rapid. Commun.* 19, 427 **(1998)**.
7. R. Verbiest, M. Kauranen, and A. J. Persoons, *J. Opt. Soc. Am. B* 15, 451 **(1998)**.
8. R. Verbiest, M. Kauranen, Y. V. Pompaey, and A. Persoons, *Phys. Rev. Lett.* 77, 1456 **(1996)**.
9. S. H. Chen, D. Katsis, A. W. Schmid, J. C. Mastrangelo, T. Tsutsui, and T. N. Blanton, *Nature* 397, 506 **(1999)**, and references there in.
10. D. Katsis, A. D. Schmid, and S. H. Chen, *Liquid Crystals* 26, 181 **(1999)**.
11. A. Marletta et al., *Macromolecules* 33, 5886 **(2000)**.

**12.** A. Marletta, D. Gonçalves, O. N. Oliveira, Jr., R. M. Faria, and F. E. G. Guimarães, *Adv. Mat.* 12, 69 (**2000**).
**13.** A. Marletta, D. Gonçalves, O. N. Oliveira, Jr., R. M. Faria, and F. E. G. Guimarães, *Macromolecules* 33, 5886 (**2000**).
**14.** A. Marletta, D. Gonçalves, O. N. Oliveira, Jr., R. M. Faria, and F. E. G. Guimarães, *Synthetic Metals* 119, 207 (**2001**).
**15.** R. B. Capaz and M. J. Caldas, *Phys. Rev. B* 67, 205205 (**2003**).
**16.** D. D. C. Bradley, *J. Phys. D: Appl. Phys.* 20, 1389 (**1987**).
**17.** A. Marletta, F. E. G. Guimarães, and R. M. Faria, *Braz. J. Phys.* 32, 570 (**2002**), and references therein.
**18.** C. R. Mendonça, D. S. dos Santos, Jr., D. T. Balogh, A. Dhanabalan, J. A. Giacometti, S. C. Zílio, and O. N. Oliveira, Jr., *Polymer* 42, 6539 (**2001**).
**19.** D. Rakovic, R. Kostic, L. A. Gribov, and I. E. Davidova, *Phys. Rev. B* 41, 10744 (**1990**).
**20.** S. Lefrant, E. Perrin, J. P. Buisson, H. Eckhardt, and C. C. Han, *Synth. Met.* 29, E91 (**1989**).
**21.** J. Cornil, D. Beljonne, C. M. Heller, I. H. Campbell, B. K. Laurich, D. L. Smith, D. D. C. Bradley, K. Mullen, and J. L. Bredas, *Chem. Phys. Lett.* 278, 139 (**1997**).
**22.** H. R. Favarin, D. Spadacio, A. D. Faceto, V. Zucolotto, O. N. Oliveira, Jr., F. E. G. Guimaraes, *Adv. Func. Mat.* 17, 28620 (**2007**).
**23.** J. R. Lakowicz, Principles of Fluorescence Spectroscopy, Kluwer Academic/Plenum Publishers, New York (**1999**).
**24.** R. M. A. Azzam, Ellipsometry and Polarized Light, North-Holland Publishing Co., Amsterdam-New York-Oxford (**1977**).
**25.** E. Collet, Polarized Light: Fundamentals and Applications, Marcel Dekker, Inc., New York, Basel, Hong Kong (**1993**).
**26.** C. S. Huang, F. S. Lu, Y. L. Li, H. Y. Gan, T. G. Liu, J. G. Xiao, X. H. Xu, S. Cui, H. B. Liu, and D. B. Zhu, *J. Nanosci. Nanotechnol.* 7, 1472 (**2007**).


Received: 28 November 2007. Accepted: 31 October 2008.